

Experimental investigation of optimal operational jet-to-target plate of multiple jet impingement heat transfer

Chukwujindu Sunday ¹, Aka Christian Chikezie ^{2,*} Onah Thomas Okechukwu ²

¹ Department of Mechanical and Production Engineering, Enugu State University of Science and Technology, Enugu, Nigeria.

² Department of Mechatronics Engineering, Enugu State University of Science and Technology, Enugu, Nigeria.

World Journal of Advanced Engineering Technology and Sciences, 2026, 18(01), 358-366

Publication history: Received on 18 December 2025; revised on 28 January 2026; accepted on 30 January 2026

Article DOI: <https://doi.org/10.30574/wjaets.2026.18.1.0044>

Abstract

Multiple jet impingement has become an established method of convectively cooling or heating surfaces in a wide multiplicity of process and thermal control applications. Impinging jets are extensively utilized in higher heat transfer applications for cooling purposes in various engineering fields such as tempering of glass and metals, heat reduction in microelectronic devices, drying of textiles and papers, gas turbine blades, aircraft deicing etc. This research work focuses on the experimental investigation of the optimal operational jet-to-target plate of multiple jet impingement heat transfer. Air jet impingement apparatus was used for the exercise. An 11×11 array with jet diameter 0.3 mm and jet-to-jet spacing of 2 mm was used to analyze the jet-to-target distance, H in the range $0.53\text{mm} \leq H \leq 3.97\text{ mm}$ at flow rates of $1.67 \times 10^{-5}\text{ m}^3/\text{s}$, $3.33 \times 10^{-5}\text{ m}^3/\text{s}$, $5 \times 10^{-5}\text{ m}^3/\text{s}$, $6.66 \times 10^{-5}\text{ m}^3/\text{s}$, $8.3 \times 10^{-5}\text{ m}^3/\text{s}$, $1 \times 10^{-4}\text{ m}^3/\text{s}$, $1.17 \times 10^{-4}\text{ m}^3/\text{s}$ and $1.33 \times 10^{-4}\text{ m}^3/\text{s}$. The array was tested by hanging it on the aluminium holder of the experimental apparatus. The heating element of wattage capacity 1000W was connected to the power source. The heater was switched on to heat the target plate. Simultaneously, heat was supplied at the bottom side of the copper plate and the blower was turned on to impinge air on the smooth and flat target plate. Air was regulated to the desired flow rate using a gate valve. The jet temperature as well as the surface temperature were measured using an infrared thermometer at every flow rate tested. Result showed that the optimum jet-to-target distance was found to be in the range $5d \leq H \leq 6d$.

Keywords: Heat Transfer Coefficient jet-to-target plate; Jet-To-Target Distances; Microelectronic devices; Round Jet Impingement

1. Introduction

Dissipation of heat has become a common cause for the thermal runaway and breakdown of several electronic devices (Tabassum et al., 2022). To effectively use these devices, it is required to extract heat from the dissipating parts. It is of utmost importance to maintain the electronic device temperature below a specified limit, as overheating may lead to performance degradation, device failure, and even operational hazards in extreme situations. For achieving higher computing efficiency, the devices must be operated in conformity to the thermal safety guidelines. Traditional air-cooling methods often fail to transfer the heat produced by such devices; this impairs the reliability and lifetime of the devices. Badr et al (2020) disclosed that multiple jet impingement is a widely implemented convective process for enhancing heat transfer over target surfaces. Impingement cooling is a method of cooling in which a cooling medium is sprayed in the form of a jet onto the surface of the cooled component in order to remove heat. The thickness of the fluid on the target cooling surface of the surface layer results in a high convection heat transfer coefficient, making this a highly stable and effective cooling method (Masip et al., 2020).

* Corresponding author: Aka Christian Chikezie.

In general, heat transfer characteristics of multi jets is different from that of the single jets. This is due to the interaction of spent air of the adjacent jets and also due to the interaction between the jets prior to impingement on the plate (Albayrak et al., 2023). Numerous studies have been reported on round jet impingement heat transfer characteristics in an array of multi jets.

Perihan et al. (2018) studied the effect of design parameters on a multi jet impinging heat transfer. The test surface is a thin metal sheet which is electrically heated and cooled using an array of nine jets arranged in inline configuration. The range of Reynolds number is 1400 to 41400. The ratio of the distance between the test sheet and nozzle exit (Z/d) is in the range of 1 to 10. The ratio of jet pitch to the jet diameter (S/d) is in the range of 2 to 10. The ratio of the distance between jet exit to the test surface (Z/d) and jet diameter in the range of 2 to 4 have significant effect on the heat transfer. The maximum heat transfer is obtained at $(S/d) = 6$. This result agrees with the result of the present study which shows that the heat transfer coefficient, h increases with increasing jet-to-target distance, H but after a jet-to-target distance of 1.45mm the heat transfer coefficient started decreasing with increasing jet-to-target distance signaling deterioration in heat transfer coefficient. When the value of jet-to-target distance is below 0.85mm deterioration in heat transfer rate also occurred. This deterioration reduces the amount of heat being transferred from the target surface. So, the optimum jet-to-target distance was found to be in the range $5 \leq H/d \leq 6$ and the maximum heat transfer which was $125000 \text{ W/m}^2 \text{ }^\circ\text{C}$ was achieved at jet-to-target distance of $5d$ and jet-to-jet spacing of $7d$ at flow rate of $1.33 \times 10^{-4} \text{ m}^3/\text{s}$.

Ren et al. (2021) conducted an experimental investigation into the jet impingement cooling. Their heated plate consisted of a high temperature co-fired ceramic material which measured $70 \text{ mm} \times 20 \text{ mm} \times 1.5 \text{ mm}$ and was placed in a square slot carved on the bottom wall of their test chamber. This was aligned with the central axis of the channel. The jets were circular with a diameter of 1.0 mm with a spacing between the jets of 1.8 mm all machined on a $20 \text{ mm} \times 100 \text{ mm}$ plate with a thickness of 2 mm. They examined the jet to crossflow velocity ratio as well as the flow and distance from the heated plate. They noted that a critical ratio does exist and that when the jet to plate distance is large, there is often a sharp degradation in the performance. They noted that the array of impinging jets when compared to a single area equivalent jet, was more effective. These results are in agreement with the results of the present study which show that the heat transfer coefficient increases with increasing jet-to-target distance but after a jet-to-target distance of 1.45mm the heat transfer coefficient started decreasing with increasing jet-to-target distance signaling deterioration in heat transfer coefficient. When the value of jet-to-target distance is below 0.85 mm deterioration in heat transfer rate also occurred. This deterioration reduces the amount of heat being transferred from the target surface. Also, the cooling performance appears to deteriorate as jet-to-target distance was increased above 3.75 mm because the cooling enhancement of the jets was having a lesser effect.

He et al. (2022) studied heat transfer enhancement of impingement cooling with corrugated target surface. The surface is electrically heated up to the initial temperature of $800 \text{ }^\circ\text{C}$. Flow rate is kept constant so that jet Reynolds number remains at $Re=24000$. Nozzle exit to surface spacing has been changed in a range of $z/d = 4-16$. For larger surface temperature drop change in nozzle exit to surface spacing does not affect the surface cooling time significantly. However, for lesser surface temperature drop particularly at higher range of surface temperature, surface cooling time is approximately 15 % higher with $z/d = 4$. The surface cooling of a hot stainless-steel surface is experimentally investigated for the stagnation point. At jet Reynolds number of 24000 and for $800 \text{ }^\circ\text{C}$ initial surface temperature it is observed that for larger drop in surface temperature, the cooling time is not affected by the change in nozzle exit to surface spacing. However, for lesser surface temperature drop particularly at higher surface temperature, surface cooling time with nozzle exit to surface spacing is approximately 15 % lower. This result is in line with the result of the present study which shows that the best effective cooling performance was achieved at a $H/d = 5$ as the target plate was cooled to $20 \text{ }^\circ\text{C}$ at flow rate of $0.000133 \text{ m}^3/\text{s}$. The cooling performance appears to deteriorate as H/d is above 13 because the cooling enhancement of the jets was having a lesser effect. Also, the Cooling performance deteriorates as H/d value was below 3 due to jet-to-target distance being so small that the jets were not forming properly reducing the amount of cooling performances.

Ikhlaq et al (2021) studied flow and heat transfer characteristics of turbulent swirling impingement jets. An experimental investigation was carried out to study the behavior of a turbulent air jet impinging on a heated plate. The study of the flow field was performed using a particle image velocimetry. A three-dimensional numerical model with Reynolds stress model has been conducted to examine the global flow. Numerical results agree well with experimental data. The main properties of the fluid occurring between the nozzle and the flat plate are presented. In addition, the effect of the distance between the nozzle exit and the plate ($h/e = 14$ and 28) were investigated and detailed analysis of the dynamic, turbulent distribution and temperature fields were performed. The wall shear stress and the pressure fields near the heated plate are then explored. Results showed that the mean velocity and the heat transfer characteristics of small nozzle-to-plate spacing are significantly different from those of large nozzle-to-plate spacing. This result agrees with the result of the present study which shows that heat transfer coefficient, h increases with

increasing jet-to-target distance, H but after a jet-to-target distance of 1.45mm the heat transfer coefficient started decreasing with increasing jet-to-target distance signaling deterioration in heat transfer coefficient. When the value of jet-to-target distance is below 0.85mm deterioration in heat transfer rate also occurred. This deterioration reduces the amount of heat being transferred from the target surface. Also, as flow rate increases

Oliveira et al. (2022) carried out experimental study of the heat transfer of single-jet impingement cooling onto a large heated plate near industrial conditions. They studied the effect of nozzle-to-plate spacing on the development of a plane jet impinging on a heated plate. The rise in separation distance resulted in decreased rate of heat transfer as the increase in the separation improves the interaction among the jets and the surroundings, and thus velocity of the jet decreases owing to increased momentum exchange. The values of coefficient of heat transfer as well as Nusselt number decline at stagnation regions. These results are in agreement with the results of the present study in which heat transfer coefficient, h increases with increasing jet-to-target distance, H but after a jet-to-target distance of 1.45mm the heat transfer coefficient started decreasing with increasing jet-to-target distance signaling deterioration in heat transfer coefficient. When the value of jet-to-target distance is below 0.85mm deterioration in heat transfer rate also occurred. This deterioration reduces the amount of heat being transferred from the target surface

Krishan, et al. (2019) studied synthetic jet impingement heat transfer enhancement- a review. They used a stainless-steel plate with the dimensions of 20 mm by 80 mm by 150 mm with an array of 9 K type thermocouples approximately 2.5 mm under the test surface placed 5 mm apart. They found that the improvement offered by jet cooling was largely not dependent on the jet velocity, rather that the system was much more sensitive to the initial temperature of the steel plate. This result is similar to the result of the present study which shows that the best effective cooling performance was achieved at a jet-to-target distance of 1.45 mm as the target plate cooled to 20 °C at flow rate of $1.33 \times 10^{-4} \text{ m}^3/\text{s}$.

Chandramohan et al. (2019) optimized heat transfer for high power electronic cooling using arrays of microjets. They experimentally and numerically examined an array of air impinging jets on a heated flat surface in the turbulent regime. Their apparatus consisted of an air inlet with an internal diameter of 21 mm and a spacing between the nozzles of 30 mm. The nozzles used had an internal diameter of 6 mm. The upper channel had an overall dimension of 36 mm × 36 mm × 230 mm and was made of Plexiglas. Their numerical model used a $k-\epsilon$ model with low Reynolds number correction for turbulence. They then used a SIMPLEC scheme to couple the velocity and pressure. They noted that decreasing the jet to target spacing resulted in an increase in the experienced heat transfer, as well as lowering the pressure drop of the system. They noted that the fluid velocity decreased as the fluid exited the jet hole resulting from the experienced shear stresses, with the velocity in the impinging region increasing with a decreasing jet to target distance. This result totally agrees with the result of the present study which shows that the local heat transfer coefficient increases as jet-to-target distance increases from 0.53 mm to 1.45 mm and starts decreasing thereafter.

Robinson and Schnitzler (2017) Studied an experimental investigation of free and submerged jet array impingement heat transfer. The heat transfer and pressure drop characteristics of jet arrays impinging on a heated surface were investigated for both confined-submerged and free-surface flow configurations. For the submerged jets it was found that the heat transfer is insensitive to changes in the jet-to-target spacing when the nozzle is in close proximity ($2 \leq H/d_n \leq 3$) to the heated surface. For the larger separation distances studied here ($5 \leq H/d_n \leq 20$) the heat transfer deteriorated monotonically with increasing jet-to-target spacing. For a fixed Reynolds number, increasing the spacing between jets also had a serious effect on the heat transfer. A stronger dependence on jet-to-jet spacing was observed for small jet-to-target spacings as compared with larger ones. The free jet configuration was found to behave thermally as a submerged jet within the range of $2 \leq H/d_n \leq 10$. Beyond this, a transition to entirely free-jet flow occurs and the heat transfer coefficient shows marginal improvement with increasing jet-to-target spacing. Consistent with previous investigation, the measurements here indicate that increasing the jet-to-jet spacing, S/d_n , causes a reduction in the heat transfer for a given Reynolds number. As compared to free-jet flows, the submerged jet configuration at small jet-to-target spacing will provide the required heat transfer coefficient with the smallest pumping power requirement. This result agrees with the result of the present study which shows that the heat transfer coefficient, h increases with increasing jet-to-target distance, H but after a jet-to-target distance of 1.45mm the heat transfer coefficient started decreasing with increasing jet-to-target distance signaling deterioration in heat transfer coefficient. When the value of jet-to-target distance is below 0.85mm deterioration in heat transfer rate also occurred. This deterioration reduces the amount of heat being transferred from the target surface. So, the optimum jet-to-target distance was found to be in the range $5 \leq H/d \leq 6$ and the maximum heat transfer which was $125000 \text{ W/m}^2 \text{ °C}$ was achieved at jet-to-target distance of $5d$ and jet-to-jet spacing of $7d$ at flow rate of $1.33 \times 10^{-4} \text{ m}^3/\text{s}$.

Ben et al. (2018) have experimentally investigated the flow and the heat transfer characteristics of a round air jet using Particle Image Velocimetry (PIV) technique. The effect of the nozzle distance ($h/d = 1$ and 2) on the dynamic characteristics and the turbulence behavior is determined. For a fixed Reynolds number, the influence of the distance

between the nozzle exit and the flat plate on the stagnation point is well captured. The authors found that when the distance increases, the separation point approaches to the jet axis increases. In addition, the results indicated that the heat transfer coefficient increases with increasing flow rate. This result agrees with the result of the present study in which jet-to-target distance, H/d increases but start reducing after H/d of 4.83.

Jung-Yang and Jenq-Jye (2018) studied the effects of jet-to-jet spacing and jet height on heat transfer characteristics of an impinging jet array. The Nusselt number distributions for five confined circular air jets vertically impinging on a flat surface were measured. The jet-to-jet spacing to jet diameter ratio (s/d) and the jet height to jet diameter ratio (H/d) were in the range of 2.0-8.0 and 0.5-3.0 respectively. The jet Reynolds number was 20,000. At small s/d and H/d values ($s/d = 2.0$ and $H/d = 0.5$), a maximum Nu , attributed to a strong flow impact (jet interaction) on the impingement plate, was clearly observed between the middle jet and every neighboring jet. The jet interaction decreases with an increase of the s/d and H/d . Jet interference before impingement causes a decrease in heat transfer. However, it achieves a uniform Nusselt number distribution in the region directly covered by the jet array. At intermediate s/d and large H/d values ($s/d = 4.0$ and $H/d = 2.0$), both the jet interaction and jet interference are weak, but the expelled air of the middle jet (cross flow) reduces the heat transfer of the neighboring jets. At large s/d values ($s/d = 6.0$), regardless of the H/d value (in the range of 0.5-3.0), every jet possesses an independent cooling area on the impingement plate.

2. Materials and Methods

2.1. Materials

The materials used in this study were copper plate of size 20 mm x 20 mm and thickness 1mm, heating element (Nichrome wire of capacity 120 V, 1 KW), air cylinder of volume 40 m³, 0.5 hp centrifugal blower, PVC pipe of 20 mm diameter, aluminum plate of thickness 3 mm, strain gage-type pressure transducer of 5 mA, 3 V dc, infrared thermometer (FLIR Lepton 3.0) and gage valve.

2.1.1. Experimental Apparatus

An experimental apparatus consists of a heater assembly, a 0.5 hp centrifugal blower, an air cylinder, PVC pipe, jet nozzle plate, flow control valves, pressure transducer, and infrared thermometer.

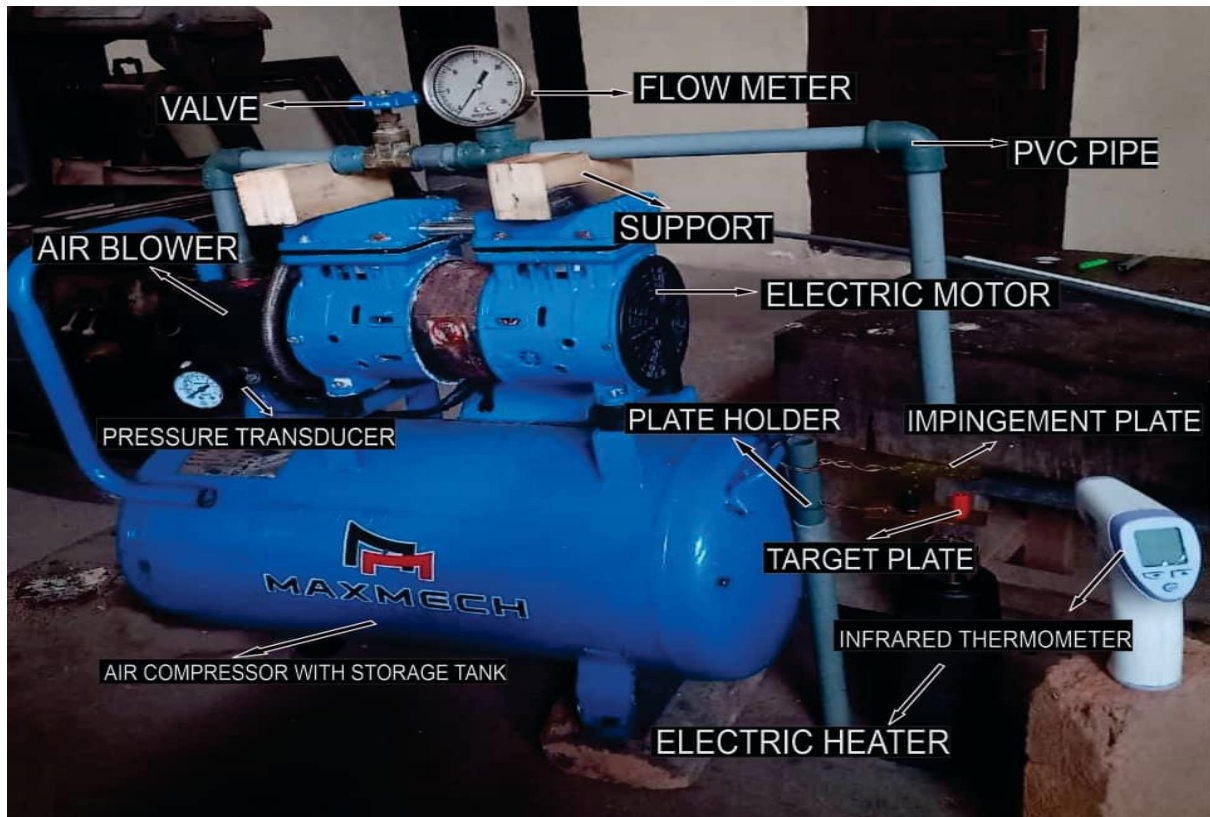


Figure 1 Experimental apparatus

A plane jet of air impinging on a heated smooth flat surface is produced by the apparatus shown in figure 1. The jet emerged from a circular nozzle (20 mm diameter). The target surface which represents the surface of a typical electronic device was made of copper, of dimensions 20 mm x 20 mm and thickness 1mm and is heated using the heater, wattage capacity of 1000 W. Copper is selected because of its high thermal conductivity. Jet nozzle plates having 0.3 mm, 0.5 mm, 0.8 mm, 1.0 mm, and 1.2 mm diameter holes were used. The holes are laser drilled and arranged in a square array of 5 x 5, 13 x 13, 14 x 14, and 16 x 16 with a jet-to-jet spacing of 2mm. The distance between the jet nozzle plate and the test plate surface is maintained at 1.45 mm. The air flow rate, and impingement plate were varied during the experiments.

2.2. Heat Transfer Measurement and Quantification

The heat transfer coefficient at the heated surface is given as (Amjadian et al., 2020).

$$h = \frac{P}{A\Delta T} = \frac{P}{A(T_s - T_j)} \quad (1)$$

Where;

- h is heat transfer coefficient ($\text{W}/\text{m}^2 \text{ }^\circ\text{C}$)
- P is heat transfer in Watts
- A is heat transfer surface area (m^2)
- T_s is target surface temperature ($^\circ\text{C}$)
- T_j is the jet temperature ($^\circ\text{C}$)

2.3. Optimal Operational Jet-to-Target Distance of a Multi-Jet Impingement Heat Transfer

The jet-to-target distance at which jet array produces the best both in cooling and in heat transfer coefficient is established as the optimal operational jet-to-target distance (Badr et al., 2025).

The jet-to-target distances used for the test are listed in table 1 while the diagram of array of eleven-jet used is shown in figure 1. An 11x11 jet arrays was tested to determine (i) the effect of jet-to-target distance on cooling performance and (ii) the effect of jet-to-target distances on heat transfer coefficient.

Table 1 Jet-to-target distances

| Letter | Test piece | H (mm) | d (mm) | H/d |
|--------|------------|--------|--------|-------|
| P | 11x11 | 0.53 | 0.3 | 1.77 |
| Q | 11x11 | 0.60 | 0.3 | 2.00 |
| R | 11x11 | 0.85 | 0.3 | 2.83 |
| S | 11x11 | 1.45 | 0.3 | 4.83 |
| T | 11x11 | 1.85 | 0.3 | 6.17 |
| U | 11x11 | 2.77 | 0.3 | 9.23 |
| V | 11x11 | 3.25 | 0.3 | 10.83 |
| W | 11x11 | 3.51 | 0.3 | 11.70 |
| X | 11x11 | 3.75 | 0.3 | 12.50 |
| Y | 11x11 | 3.97 | 0.3 | 13.23 |

Table 1 shows letters P, Q, R, S, T, U, V, W, X, Y with jet-to-target distances of 0.53 mm, 0.60 mm, 1.85 mm, 2.77 mm, 3.25 mm, 3.51 mm, 3.75 mm, and 3.97 mm respectively, that have same array 11 x 11 and same diameter 0.3 mm. The arrays were tested to determine the effect of jet-to-target distance on cooling efficient and heat transfer performance.

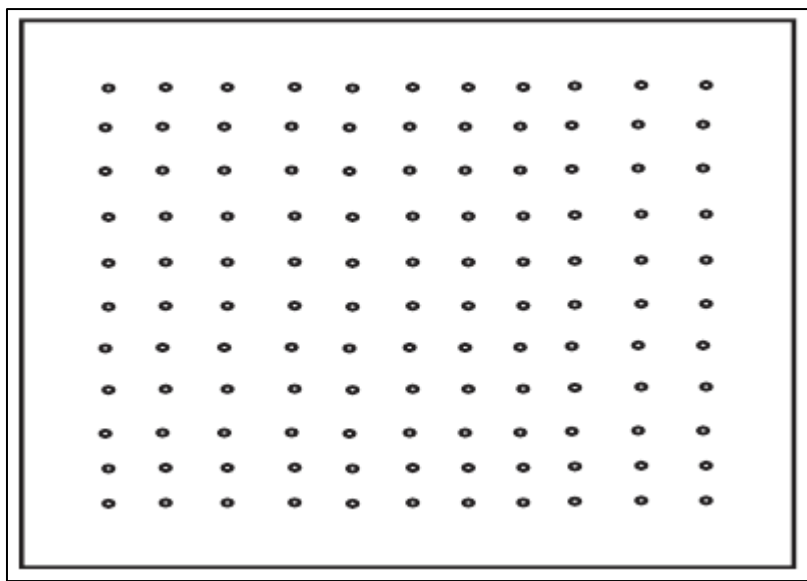


Figure 2 An 11×11 array with 0.3 mm jets diameter spaced at 2mm.

Figure 2 shows 11×11 array with jet diameter and jet spacing of 0.3 mm and 2 mm respectively used to analyze the effect of jet-to-target distances on cooling efficient and heat transfer performance.

2.4. Experimental Procedure

We started by hanging an 11×11 array with jet diameter and jet spacing of 0.3 mm and 2 mm respectively on an aluminium holder at a jet-to-target distance of 0.53 mm, and connected the heating element to the power source with current and voltage maintained at 8.3 A and 120 V respectively. The heater was switched on to heat the target plate. Instantaneously, heat was supplied at the bottom side of the plate and except top surface other sides were insulated perfectly using electrical insulating material to prevent electrical contact of the heater with the plate and the blower was turned on to impinge air on the smooth and flat target plate. We ensured that air was regulated to the desired flow rate using gate valve. We captured the jet temperature, T_j before the air impinges on the target plate and captured also the surface temperature, T_s after the target plate had reached a steady state using infrared thermometer. Temperature change, ΔT that is $(T_s - T_j)$ was calculated and equation 1 was used to calculate the heat transfer coefficient.

We continued the experiment with the same 11×11 array till every jet-to-target distance, H listed in table 1 was tested at flow rate of $1.67 \times 10^{-5} \text{ m}^3/\text{s}$, $3.33 \times 10^{-5} \text{ m}^3/\text{s}$, $5 \times 10^{-5} \text{ m}^3/\text{s}$, $6.66 \times 10^{-5} \text{ m}^3/\text{s}$, $8.3 \times 10^{-5} \text{ m}^3/\text{s}$, $1 \times 10^{-4} \text{ m}^3/\text{s}$, $1.17 \times 10^{-4} \text{ m}^3/\text{s}$ and $1.33 \times 10^{-4} \text{ m}^3/\text{s}$. At each test performed, the required parameters were noted, calculated and results tabulated.

3. Results and discussion

3.1. Optimal Operational Jet-to-Target Distance of a Multi-Jet Impingement Heat Transfer.

The result of the optimal operational jet-to-target distance of a multi- jet impingement heat transfer is explained in the following sessions.

3.1.1. Effect of jet-to-target distance on cooling performance.

The temperature rise against jet-to-target distances of 0.53 mm, 0.6 mm, 0.85 mm, 1.45 mm, 1.85 mm, 2.77 mm, 3.25 mm, 3.51 mm, 3.75 mm and 3.95 mm at flow rates of $1.67 \times 10^{-5} \text{ m}^3/\text{s}$, $3.33 \times 10^{-5} \text{ m}^3/\text{s}$, $5 \times 10^{-5} \text{ m}^3/\text{s}$, $6.66 \times 10^{-5} \text{ m}^3/\text{s}$, $8.3 \times 10^{-5} \text{ m}^3/\text{s}$, $1 \times 10^{-4} \text{ m}^3/\text{s}$, $1.17 \times 10^{-4} \text{ m}^3/\text{s}$ and $1.33 \times 10^{-4} \text{ m}^3/\text{s}$ is shown in figure 2. Result showed that the best effective cooling performance was achieved at a jet-to-target distance of 1.45mm because the target plate cooled to 49 °C, 43 °C, 39 °C, 35 °C, 32 °C, 27 °C, 24 °C, 20 °C at flow rates of $1.67 \times 10^{-5} \text{ m}^3/\text{s}$, $3.33 \times 10^{-5} \text{ m}^3/\text{s}$, $5 \times 10^{-5} \text{ m}^3/\text{s}$, $6.66 \times 10^{-5} \text{ m}^3/\text{s}$, $8.3 \times 10^{-5} \text{ m}^3/\text{s}$, $1 \times 10^{-4} \text{ m}^3/\text{s}$, $1.17 \times 10^{-4} \text{ m}^3/\text{s}$, $1.33 \times 10^{-4} \text{ m}^3/\text{s}$ respectively. The second best effective cooling performance was achieved at a jet-to-target distance of 1.85 mm at which the target plate cooled to 52 °C, 45.15 °C, 40 °C, 36.87 °C, 34 °C, 30 °C, 27 °C, 22 °C at flow rates of $1.67 \times 10^{-5} \text{ m}^3/\text{s}$, $3.33 \times 10^{-5} \text{ m}^3/\text{s}$, $5 \times 10^{-5} \text{ m}^3/\text{s}$, $6.66 \times 10^{-5} \text{ m}^3/\text{s}$, $8.3 \times 10^{-5} \text{ m}^3/\text{s}$, $1 \times 10^{-4} \text{ m}^3/\text{s}$, $1.17 \times 10^{-4} \text{ m}^3/\text{s}$ and $1.33 \times 10^{-4} \text{ m}^3/\text{s}$ respectively. The result also showed that cooling performance appears to deteriorate as jet-to-target distance was increased above 3.75 mm because the cooling enhancement of the jets was

having a lesser effect. Result also showed that the Cooling performance deteriorate also as the jet-to-target distance was decreased below 0.85 mm due to the jet-to-target distance being so small that the jets were not forming properly reducing the amount of cooling performances. The jet-to-target distance of 1.45mm is approximately 5 jet diameters whereas the jet-to-target distance of 1.85 mm is about 6 jet diameters. Therefore, the optimum jet-to target distance is found to be in the range $1.45\text{mm} \leq H \leq 1.85\text{ mm}$ or $5d \leq H \leq 6d$ or $5 \leq H/d \leq 6$. The pressure drops as well as the pumping power requirement across the test pieces increases as jet-to-target distance decreases. These results are in agreement with the results of research done by (He et al., 2022; Krishan et al., 2019),

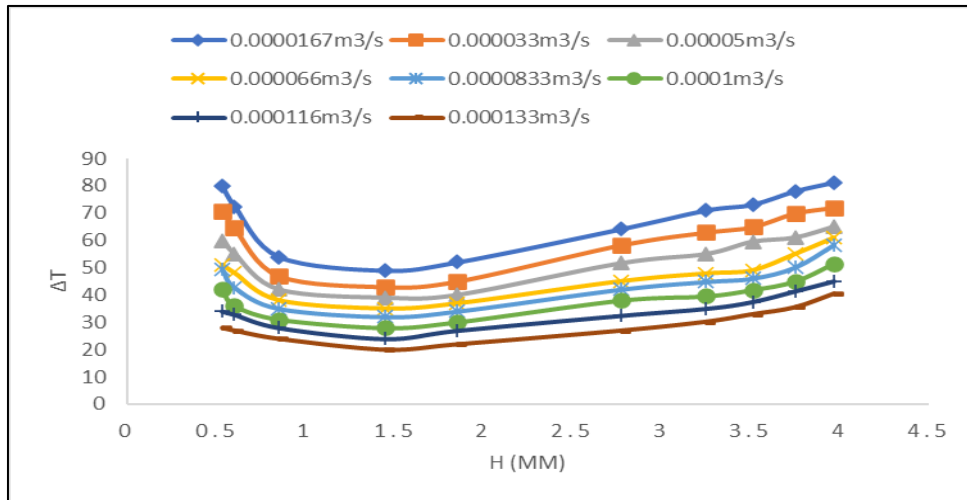


Figure 3 Temperature rise against jet-to target distance

3.1.2. Effect of jet-to-target distance on heat transfer coefficient.

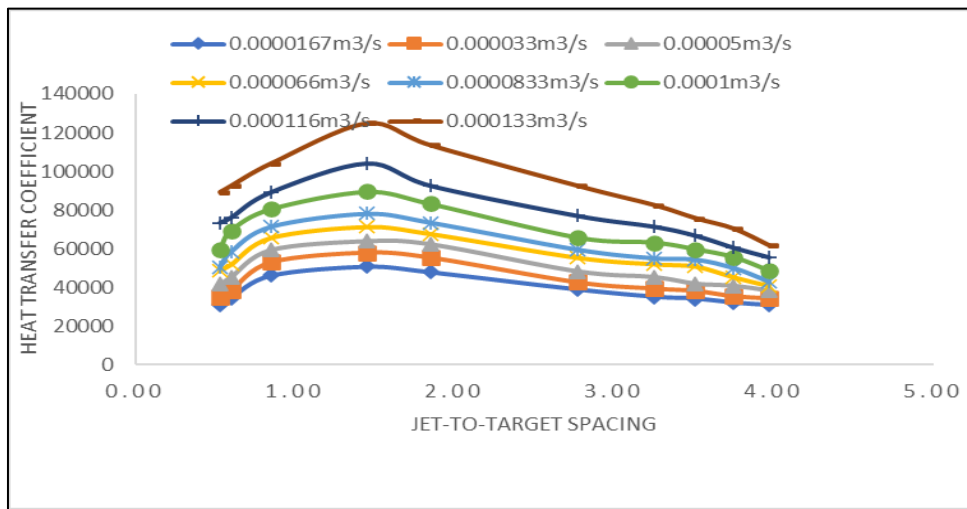


Figure 4 Heat transfer coefficient against jet-to-target distance

The heat transfer coefficient against at jet-to-target distances of 0.53 mm, 0.6 mm, 0.85 mm, 1.45 mm, 1.85 mm, 2.77 mm, 3.25 mm, 3.51 mm, 3.75 mm and 3.95 mm at flow rates of $1.67 \times 10^{-5} \text{ m}^3/\text{s}$, $3.33 \times 10^{-5} \text{ m}^3/\text{s}$, $5 \times 10^{-5} \text{ m}^3/\text{s}$, $6.66 \times 10^{-5} \text{ m}^3/\text{s}$, $8.3 \times 10^{-5} \text{ m}^3/\text{s}$, $1 \times 10^{-4} \text{ m}^3/\text{s}$, $1.17 \times 10^{-4} \text{ m}^3/\text{s}$ and $1.33 \times 10^{-4} \text{ m}^3/\text{s}$ is shown in figure 4. Result showed that when these jet-to-target distances were compared that the best heat transfer coefficient was achieved at a jet-to-target distance of 1.45mm. The heat transfer coefficients were $51020 \text{ W/m}^2 \text{ }^\circ\text{C}$, $58140 \text{ W/m}^2 \text{ }^\circ\text{C}$, $64103 \text{ W/m}^2 \text{ }^\circ\text{C}$, $71427 \text{ W/m}^2 \text{ }^\circ\text{C}$, $78125 \text{ W/m}^2 \text{ }^\circ\text{C}$, $89638 \text{ W/m}^2 \text{ }^\circ\text{C}$, $104167 \text{ W/m}^2 \text{ }^\circ\text{C}$ and $125000 \text{ W/m}^2 \text{ }^\circ\text{C}$ at flow rates of $1.67 \times 10^{-5} \text{ m}^3/\text{s}$, $3.33 \times 10^{-5} \text{ m}^3/\text{s}$, $5 \times 10^{-5} \text{ m}^3/\text{s}$, $6.66 \times 10^{-5} \text{ m}^3/\text{s}$, $8.3 \times 10^{-5} \text{ m}^3/\text{s}$, $1 \times 10^{-4} \text{ m}^3/\text{s}$, $1.17 \times 10^{-4} \text{ m}^3/\text{s}$ and $1.33 \times 10^{-4} \text{ m}^3/\text{s}$ respectively. The second best heat transfer coefficient was achieved at a jet-to-target distance of 1.85mm, at which the heat transfer coefficients were $48077 \text{ W/m}^2 \text{ }^\circ\text{C}$, $53371 \text{ W/m}^2 \text{ }^\circ\text{C}$, $62500 \text{ W/m}^2 \text{ }^\circ\text{C}$, $67806 \text{ W/m}^2 \text{ }^\circ\text{C}$, $73529 \text{ W/m}^2 \text{ }^\circ\text{C}$, $83333 \text{ W/m}^2 \text{ }^\circ\text{C}$, $92593 \text{ W/m}^2 \text{ }^\circ\text{C}$ and $113636 \text{ W/m}^2 \text{ }^\circ\text{C}$ at flow rates of $1.67 \times 10^{-5} \text{ m}^3/\text{s}$, $3.33 \times 10^{-5} \text{ m}^3/\text{s}$, $5 \times 10^{-5} \text{ m}^3/\text{s}$, $6.66 \times 10^{-5} \text{ m}^3/\text{s}$, $8.3 \times 10^{-5} \text{ m}^3/\text{s}$, $1 \times 10^{-4} \text{ m}^3/\text{s}$, $1.17 \times 10^{-4} \text{ m}^3/\text{s}$ and $1.33 \times 10^{-4} \text{ m}^3/\text{s}$ respectively. The heat transfer coefficient, h increases with

increasing jet-to-target distance, H but after a jet-to-target distance of 1.45 mm the heat transfer coefficient started decreasing with increasing jet-to-target distance signaling deterioration in heat transfer coefficient. When the value of jet-to-target distance is below 0.85 mm deterioration in heat transfer rate also occurred. This deterioration reduces the amount of heat being transferred from the target surface. The jet-to-target distance of 1.45 mm is approximately 5 jet diameters whereas the jet-to-target distance of 1.85 mm is about 6 jet diameters. Therefore, the optimum jet-to-target distance was found to be in the range $1.45 \text{ mm} \leq H \leq 1.85 \text{ mm}$ or $5d \leq H \leq 6d$ or $5 \leq H/d \leq 6$. The result is in line with the result obtained by (Fenot et al., 2021; Ren et al., 2021; Ikhlaq et al., 2021; Oliveira et al., 2022).

Nomenclature

- A : Heat transfer surface area: (m^2)
- d : Jet diameter: (mm)
- h : Heat transfer coefficient: ($\text{W}/\text{m}^2 \text{ }^\circ\text{C}$)
- P : Power; (W)
- T : Temperature of the jet :($^\circ\text{C}$)
- T_s : Temperature of the surface: ($^\circ\text{C}$)
- Q : Volume flow rate:(m^3/s)

4. Conclusion

The present study provides a good understanding of cooling performance and heat transfer characteristics of air impinging jets. Experiments were conducted to determine the effect of jet-to-target distance on cooling efficient and heat transfer coefficient performances. Results showed that the optimum jet-to-target distance was found to be in the range $5d \leq H \leq 6d$, the maximum heat transfer which was $125000 \text{ W}/\text{m}^2 \text{ }^\circ\text{C}$ was achieved at jet-to-target distance of $5d$ and jet-to-jet spacing of $7d$ as the target plate cooled to $20 \text{ }^\circ\text{C}$ at flow rate of $1.33 \times 10^{-4} \text{ m}^3/\text{s}$.

Compliance with ethical standards

Disclosure of conflict of interest

No conflict of interest to be disclosed.

References

- [1] Albayrak M, Sarper B, Saglam M, Birinci S, Aydin O. (2023). The role of jet-to-crossflow velocity ratio on convective heat transfer enhancement in the cooling of discrete heating modules. *Thermal Science and Engineering Progress*, 37, 101549.
- [2] Badr, M. A., Lioua, K., & Hacen, D. (2020). CFD analysis of heat transfer enhancement in impinging jet array by varying number of jets and spacing. *International Journal of Gas Turbine, Propulsion and Power Systems*, 4, 23-37.
- [3] Ben, K. R., Habli, R., Mahjoub, S. N., Bournot, H., & Le, P. G. (2018). Parametric analysis of a round jet impingement on a heated plate. *International Journal of Heat Fluid Flow*, 57, 11-23.
- [4] Chandramohan, P., Murugesan, S. N., & Arivazhagan, S. (2019). Experimental investigation and CFD analysis of influence of swirl, arrangement of nozzle, cross section and diameter of jets on heat transfer in multi-jet air impingement cooling. *Journal of Thermal Science*, 23, 25-35.
- [5] He, J., Deng, Q., & Feng, Z. (2022). Heat transfer enhancement of impingement cooling with corrugated target surfaces. *International Journal of Thermal Science*, 17, 91-123.
- [6] Ikhlaq, M., Al-Abdeli, Y. M., & Khiadani, M. (2021). Flow and heat transfer characteristics of turbulent swirling impingement jets. *Appl. Therm. Eng.*, 196, 20-30.
- [7] Jung-Yang, S., & Jenq-Jye, C. (2018). Effect of jet-to-jet spacing and jet height on heat transfer characteristics of an impinging jet array. *Elsevier Ltd*.
- [8] Krishan, G., & Sharma, R. N. (2019). Synthetic jet impingement heat transfer enhancement. A review. *Appl. Therm. Eng.*, 149, 305-323.

- [9] Masip, Y., Campo, A., & Nunez, S. M. (2020). Experimental analysis of the thermal performance on electronic cooling by a combination of cross-flow and an impinging air jet. *Applied Thermal Engineering*, 167, 45-57.
- [10] Oliveira, A. V. S., Marechal, D., Borean, J. L., Schick, V., Denis, S., & Gradeck, M. (2022). Experimental study of the heat transfer of single-jet impingement cooling onto a large heated plate near industrial conditions. *Int. J. Heat Mass Transf.*, 47, 231- 243.
- [11] Perihan, C., Nevin, C., & Kazim, P. (2018). Effect of design parameters on a multi-jet impinging heat transfer. *Alexandria Engineering Journal*, 34, 78-111.
- [12] Ren, X., Yang, X., Lu., X., Li, X., & Ren, J. (2021). Experimental investigation of micro cooling units on impingement jet array flow pressure loss and heat transfer characteristics. *International Journal of Heat and Mass Transfer*, 14(16), 87-101.
- [13] Robinson, A. J., & Schnitzler, E. (2017). An experimental investigation of free and submerged miniature liquid jet array impingement heat transfer. *Journal of Heat and Mass Transfer*, 25, 126-135.
- [14] Tabassum, S., Hilfer, M., Brakmann, R. G., Willert, C. M. C., Matha, M., & Schroll, M. (2022). Validation and assessment of computational fluid dynamic modeling of multi-jet impingement cooling with the experiments. *In ASME Turbo Expo. Turbomachinery Technical Conference and Exposition*, 12